TGF-β signaling is essential for joint morphogenesis

Anna Spagnoli,[1,3] Lynda O'Rear,[1] Ronald L. Chandler,[2] Froilan Granero-Molto,[1] Douglas P. Mortlock,[2] Agnieszka E. Gorska,[3] Jared A. Weis,[1] Lara Longobardi,[1] Anna Chytil,[3] Kimberly Shimer,[1] and Harold L. Moses[3]

[1]Department of Pediatrics, [2]Department of Molecular Physiology and Biophysics, and [3]Department of Cancer Biology, Vanderbilt University School of Medicine, Nashville, TN 37232

Despite its clinical significance, joint morphogenesis is still an obscure process. In this study, we determine the role of transforming growth factor β (TGF-β) signaling in mice lacking the TGF-β type II receptor gene (*Tgfbr2*) in their limbs (*Tgfbr2*$^{PRX\text{-}1KO}$). In *Tgfbr2*$^{PRX\text{-}1KO}$ mice, the loss of TGF-β responsiveness resulted in the absence of interphalangeal joints. The *Tgfbr2*^{Prx1KO} joint phenotype is similar to that in patients with symphalangism (SYM1-OMIM185800). By generating a *Tgfbr2–green fluorescent protein–β–GEO–bacterial artificial chromosome* β-galactosidase reporter transgenic mouse and by in situ hybridization and immunofluorescence, we determined that *Tgfbr2* is highly and specifically expressed in developing joints. We demonstrated that in *Tgfbr2*$^{PRX\text{-}1KO}$ mice, the failure of joint interzone development resulted from an aberrant persistence of differentiated chondrocytes and failure of Jagged-1 expression. We found that TGF-β receptor II signaling regulates *Noggin*, *Wnt9a*, and *growth and differentiation factor-5* joint morphogenic gene expressions. In *Tgfbr2*$^{PRX\text{-}1KO}$ growth plates adjacent to interphalangeal joints, *Indian hedgehog* expression is increased, whereas *Collagen 10* expression decreased. We propose a model for joint development in which TGF-β signaling represents a means of entry to initiate the process.

Introduction

In industrialized countries, osteoarthritis affects more than one third of the adult population. Despite their clinical importance, the molecular mechanisms of joint morphogenesis are still unclear. The appendicular skeleton arises from the condensation of chondroprogenitor cells that undergo chondrocyte template formation that is subsequently replaced by bone to form the adult skeletal elements separated by cartilaginous joints. The synovial joints of the long bone elements form through segmentation of the continuous cartilaginous template with loss at the sites of the developing joints, loss of differentiated chondrocytes, and emergence of a nonchondrocytic joint-forming cell population that undergoes condensation, flattens, and develops an interzone that then cavitates to form the joint space within the articular cartilage (for review see Archer et al., 2003). There is limited information on the mechanisms that regulate the complex multistep process that leads to joint interzone formation. In fact, very few genes have been reported to be necessary and/or sufficient to initiate the joint formation process (namely *Noggin*, *growth and differentiation factor-5* [*Gdf-5*], and *Wnt9a* [previously known as *Wnt14*]; Storm et al., 1994; Brunet et al., 1998; Hartmann and Tabin, 2001). The factors that induce the expression of these joint morphogenic molecules are undefined; furthermore, the mechanisms that determine the emergence of joint interzone cells within the chondrogenic condensates are unclear.

TGF-βs elicit their signal binding to TGF-β type II receptor (TβRII) that leads to the phosphorylation of TβRI and TβRII–TβRI complex formation, which then activates the signaling cascade through R-Smad–dependent (Smad-2,-3,-4) and Smad-independent pathways. In human and mouse embryonic cartilage, TGF-βs are expressed in the endochondral template with high expression in the perichondrium (Millan et al., 1991; Pelton et al., 1991a,b; Lawler et al., 1994; Serra and Chang, 2003). TβRI and TβRII have been reported to be expressed in the perichondrium and proliferative and differentiated chondrocytes (Serra and Chang, 2003).

Genetic manipulation of the TGF-β system genes have revealed their critical but still undefined roles in skeletogenesis (Serra et al., 1997; Ito et al., 2003; Baffi et al., 2004; for review see Dunker and Krieglstein, 2000). Targeted germline deletion of the *Tgfb2* gene in mice results in perinatal lethality, and mice

Correspondence to Anna Spagnoli: anna.spagnoli@vanderbilt.edu

Abbreviations used in this paper: BAC, bacterial artificial chromosome; BMP, bone morphogenic protein; DNIIR, dominant-negative *Tgfbr2*; GDF-5, growth and differentiation factor-5; Ihh, Indian hedgehog; LCM, laser capture microdissection; micro-CT; microcomputed tomography; PTH-rP, parathyroid hormone–related protein; TβR, TGF-β receptor; WIB, Western immunoblotting.

The online version of this article contains supplemental material.

The Journal of Cell Biology, Vol. 177, No. 6, June 18, 2007 1105–1117
http://www.jcb.org/cgi/doi/10.1083/jcb.200611031

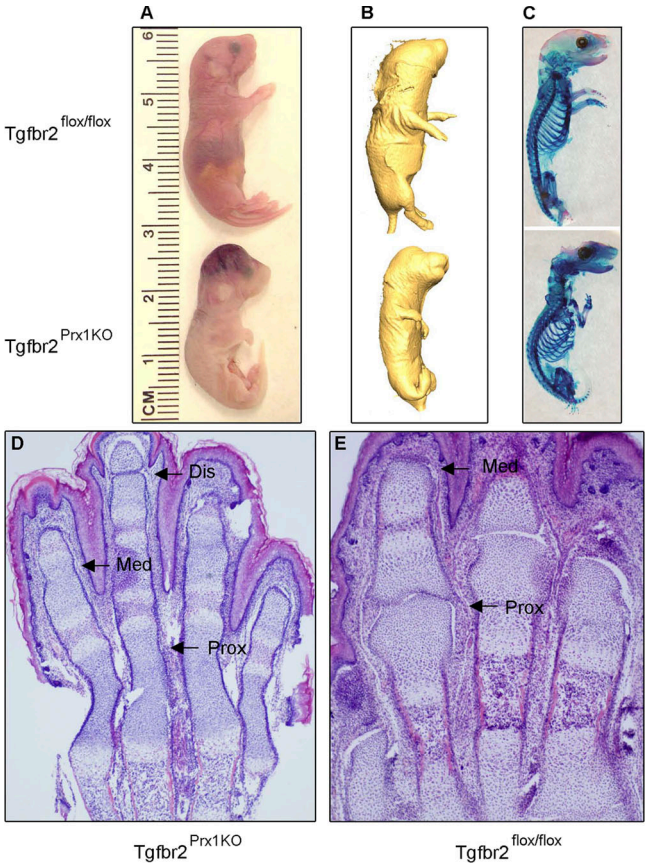

Figure 1. **TGF-β signaling regulates limb development and is essential for interphalangeal joint formation.** (A–C) External morphology (A), micro-CT analysis (B), and Alizarin red/Alcian blue staining of newborn *Tgfbr2*^{Prx1KO} mutant (C, bottom) and *Tgfbr2*$^{flox/flox}$ control (C, top) demonstrating that the mutant is smaller and has severe stylopod, zeugopod, and autopod defects. (D and E) Morphometric analysis of sectioned autopod forelimbs of newborn *Tgfbr2*^{Prx1KO} mutant (D) and *Tgfbr2*$^{flox/flox}$ control (E) by hematoxylin and eosin, indicating that the mutant lacked the proximal (Prox) and medial (Med) interphalangeal joints; sporadically, a distal interphalangeal joint (Dis) is observed (as in the third digit).

present several skeletal defects, including cleft palate, skull ossification defects, shortened long bones, bifurcation of the sternum, and spina bifida occulta (Sanford et al., 1997). 50% of the *Tgfb1* ablated mice die early in utero before embryonic day (E) 10.5 because of a preimplantation defect; mice that are born do not display any dysmorphic phenotype but die early from diffuse inflammation (Shull et al., 1992; for review see Dunker and Krieglstein, 2000). *Tgfb3*-null mice have cleft palate and abnormal lungs (Kaartinen et al., 1995). Variability in the skeletal phenotype in *Tgfb*-targeted disrupted mice can be the result of differential and overlapping expression patterns of the isoforms throughout the skeletogenesis process and, therefore, compensatory effects of the other isoforms when one is ablated. Similarly, *R-Smad* gene targeting in mice has lead to variable phenotypes from early lethality (*Smad-2* and *Smad-4* ablation) to normal phenotype at birth but progressive osteoarthritis and colon adenocarcinomas in adulthood (*Smad-3* ablation; Sirard et al., 1998; Weinstein et al., 1998; Zhu et al., 1998; Yang et al., 2001). TβRII is the only TβR that is capable of binding all of the TGF-β isoforms and eliciting functional signaling; therefore, its ablation will allow studies of TGF-β signaling that avoid the functional redundancy of the ligands and signaling pathways. Unfortunately, mice that are germline null for *Tgfbr2* exhibit early embryonic lethality that makes it impossible to evaluate the role of TGF-β signaling in skeletogenesis (Oshima et al., 1996). We have previously reported that in transgenic mice, overexpression of a dominant-negative *Tgfbr2* (DNIIR) results in adult osteoarthritis (Serra et al., 1997). However, the phenotype was only observed in a few lines, most likely because expression was inconsistent and lacked tissue-specific targeting (Serra et al., 1997). Furthermore, the TGF-β cell targets and the temporal window of essential function during the endochondral process are not well defined. Conditional inactivation of *Tgfbr2* in differentiated chondrocytes results in mice without any long bone defects, leading to the conclusion that TGF-β signaling is not needed in the limb endochondral process (Baffi et al., 2004). However, implanted TGF-β induces extra digit formation (Ganan et al., 1996). To circumvent the embryonic lethality of *Tgfbr2* systemic ablation and to determine the role of TGF-β signaling in early limb bud development, we generated mice in which the TβRII signaling is conditionally inactivated in limb buds and in a subset of other mesenchyme tissues starting at E9.5 (*Tgfbr2*$^{PRX\text{-}1KO}$).

We show that in Tgfbr2PRX-1KO mice, TGF-β signaling ablation results in the following: (1) lack of interphalangeal joint development; (2) failure of joint interzone formation with a lack of Jagged-1 expression and aberrant survival of differentiated chondrocytes that leads to the absence of segmentation within the chondrogenic condensates; (3) failure of joint morphogenic marker expression, including Noggin, and increased bone morphogenic protein (BMP) activity in limb bud cultures; (4) a selective defect on the endochondral growth plate process adjacent to the interphalangeal joints at early and late chondrogenesis with an increase of prehypertrophic chondrocyte markers and a decrease of terminally differentiated chondrocyte marker expression; and (5) midline defects and zeugopod and stylopod chondrodysplasia. Furthermore, using a TβRII reporting mouse and in situ and immunohistochemistry analyses, we have demonstrated that TβRII is highly and specifically expressed in developing joints.

Results

TGF-β signaling is needed for joint development and to regulate midline and limb skeletogenesis

To conditionally inactivate the TGF-β signaling in limb buds, we crossed *Tgfbr2*$^{flox/flox}$ homozygous females with *Prx1-Cre*(Cre^{+});*Tgfbr2*^{flox} double heterozygous males (Cre^{+}Tgfbr2$^{flox/-}$) to generate *Tgfbr2*^{Prx1KO} mice (homozygous knockouts). Newborn *Tgfbr2*^{Prx1KO} mice showed abnormal forelimbs and hindlimbs (Fig. 1 A), which were confirmed by microcomputed tomography (micro-CT) imaging and Alizarin red/Alcian blue staining (Fig. 1, B and C). *Tgfbr2*^{Prx1KO} autopods lacked interphalangeal joint development, and, between the ossification centers of the phalanges, at the site where the joints should have been formed, there was a continuous pattern of cells with some bending,

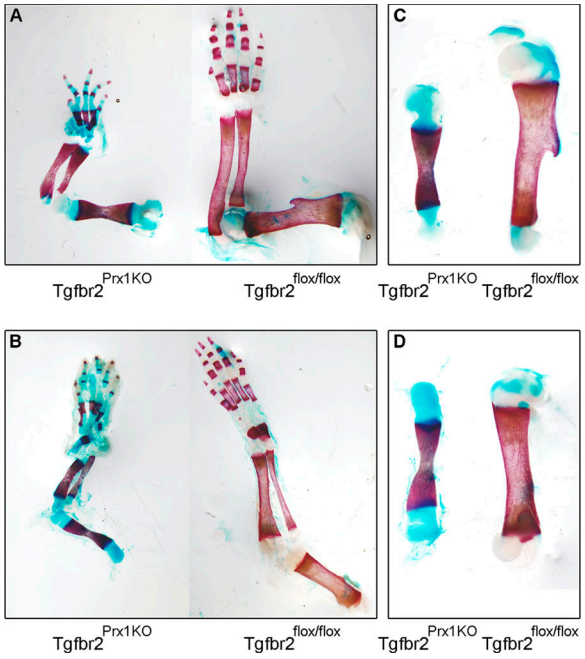

Figure 2. **TGF-β signaling regulates the morphological features of limb stylopods, zeugopods, and autopods.** (A–D) Alizarin red/Alcian blue limb skeletons were prepared from newborn *Tgfbr2*^{Prx1KO} mutants and *Tgfbr2*$^{flox/flox}$ control mice. Mutants (left) showed smaller forelimbs (A) and hindlimbs (B) with bended zeugopods and autopods. *Tgfbr2*^{Prx1KO} humerus and femur stylopods (C and D) were shorter, had a middle concavity, and showed dysplastic poorly mineralized metaphyses. Humerus (C) lacked the deltoid tuberosity.

and a distal interphalangeal joint was seen sporadically (Fig. 1, D and E). Forelimb and hindlimb interphalangeal joints were equally affected, and studies were performed either on forelimbs or hindlimbs, but mostly on both. The *Tgfbr2*^{Prx1KO} forelimb and hindlimb autopods displayed smaller ossification centers of the metacarpals, carpals, metatarsals, tarsals, and phalanges as compared with controls; phalanges were bent (clinodactyly; Fig. 2, A and B). *Tgfbr2*^{Prx1KO} zeugopods and stylopods were short with signs of chondrodysplasia (Fig. 2, A and B). The humerus lacked the deltoid tuberosity and, similar to the femur, had dysplastic widened, flaring, and poorly mineralized metaphyses (Fig. 2, C and D).

The morphometric parameters of newborn *Tgfbr2*^{Prx1KO} mutants are summarized in Table I. Compared with control Cre^{-} siblings, mutants are shorter, and their length is more affected than their weight, as demonstrated by the higher ponderal index. This finding indicates that in *Tgfbr2*^{Prx1KO} mutants, the skeletal growth is impaired by a primary defect on skeletogenesis and is not the result of a global intrauterine nutritional defect.

Tgfbr2^{Prx1KO} mice had several midline defects: they lacked sternum formation, had hypoplastic incisors, and lacked the parietal and interparietal bones, whereas the frontal and squamosal bones were reduced in size (Fig. 3, A–J). They were capable of suckling, but they experienced massive and progressively visible intracranial bleeding (although still alive) that, at the necropsy exam, occupied most of the brain and likely was the primary cause of death. Although it is possible that a respiratory insufficiency caused by the lack of the sternum may be a concomitant cause of death, it is unlikely to be the primary cause considering the severity of the intracranial bleeding. Lack of parietal and interparietal bone development was confirmed by micro-CT analyses of living newborn *Tgfbr2*^{Prx1KO} mice, indicating that loss was not caused by accidental removal of the vault during the Alizarin red/Alcian blue staining procedure (Fig. 3, I and J). The pelvic bones of *Tgfbr2*^{Prx1KO} mice were smaller and poorly mineralized with signs of chondrodyplasia (Fig. 3, E and F).

Because we observed skeletal defects in segments unexpected for the reported Prx-1–mediated Cre recombination, we decided to evaluate the Prx1-Cre expression pattern in *Tgfbr2*^{Prx1KO} mice by crossing females doubly homozygous for *Tgfbr2*$^{flox/flox}$ and R26R loci (*Tgfbr2*$^{flox/flox}$-R26R) with males heterozygous for *Prx1-Cre* to generate *Tgfbr2*^{Prx1KO}-R26R mice. In the R26R mice, the ROSA26 locus is targeted by gene trapping

Table I. **Newborn morphometric parameters in *Tgfbr2*^{prx1KO} and control Cre^{-} siblings (Tgfbr2$^{flox/flox}$;Tgfbr2$^{flox/-}$)**

	Genotype	*n*	Mean ± SD	P-value
Body length (cm)	*Tgfbr2*^{prx1KO}	9	2.52 ± 0.17	0.0039
	Tgfbr2$^{flox/flox}$;*Tgfbr2*$^{flox/-}$	17	3.00 ± 0.28	
Body weight (g)	*Tgfbr2*^{prx1KO}	9	1.15 ± 0.08	0.0362
	Tgfbr2$^{flox/flox}$;*Tgfbr2*$^{flox/-}$	17	1.52 ± 0.37	
Ponderal index (g/cm^3)	*Tgfbr2*^{prx1KO}	9	7.37 ± 1.84	0.0086
	Tgfbr2$^{flox/flox}$;*Tgfbr2*$^{flox/-}$	17	5.70 ± 1.14	
Humerus length (cm)	*Tgfbr2*^{prx1KO}	4	0.28 ± 0.03	0.004
	Tgfbr2$^{flox/flox}$;*Tgfbr2*$^{flox/-}$	8	0.51 ± 0.02	
Radius length (cm)	*Tgfbr2*^{prx1KO}	4	0.15 ± 0.02	<0.0001
	Tgfbr2$^{flox/flox}$;*Tgfbr2*$^{flox/-}$	8	0.39 ± 0.01	
Ulna length (cm)	*Tgfbr2*^{prx1KO}	4	0.22 ± 0.008	0.004
	Tgfbr2$^{flox/flox}$;*Tgfbr2*$^{flox/-}$	8	0.49 ± 0.007	
Femur length (cm)	*Tgfbr2*^{prx1KO}	4	0.33 ± 0.01	<0.0001
	Tgfbr2$^{flox/flox}$;*Tgfbr2*$^{flox/-}$	8	0.45 ± 0.03	
Tibia length (cm)	*Tgfbr2*^{prx1KO}	4	0.25 ± 0.005	0.004
	Tgfbr2$^{flox/flox}$;*Tgfbr2*$^{flox/-}$	8	0.45 ± 0.02	

Body lengths (from the tip of the nose to the anus) were measured on anesthetized animals stretched on top of a ruler. Ponderal indexes were calculated using the formula of Roher as weight (grams)/(length [centimeters])^3 × 100 (Rohrer, 1921). Stylopod and zeupod lengths were measured in Alizarin red/Alcian blue–stained elements.

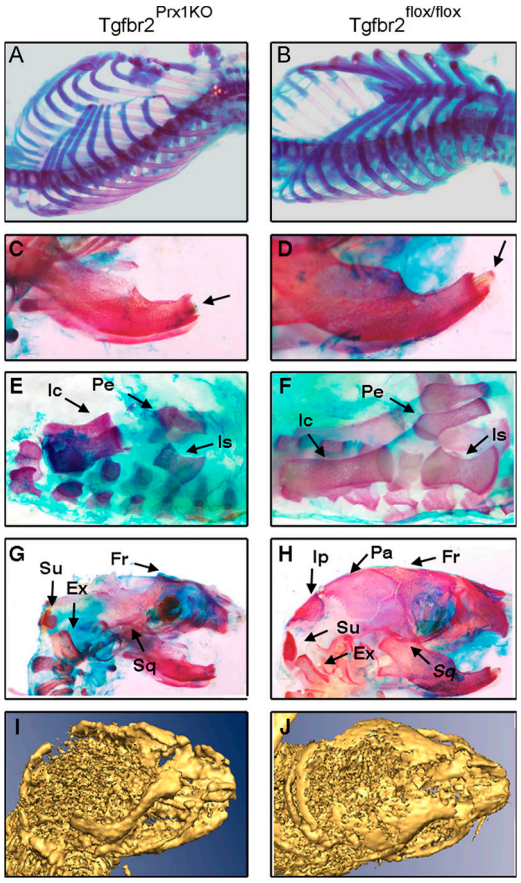

Figure 3. **Lack of TGF-β signaling determines axial, pelvic bones, and calvaria defects.** (A–H) Alizarin red/Alcian blue ribcage (A and B), mandibular (C and D), pelvis (E and F), and calvaria (G and H) skeletons were prepared from newborn *Tgfbr2*^{Prx1KO} mutants and *Tgfbr2*$^{flox/flox}$ control mice. In *Tgfbr2*^{Prx1KO} mice, the ribcage is open, lacking sternum development (A); the incisors were hypoplastic (C), and the ischial (Is), pelvic (Pe), and iliac (Ic) bones (marked by arrows) were smaller and chondrodysplastic (D). *Tgfbr2*^{Prx1KO} mice lacked the parietal (Pa) and interparietal (Ip) bones, whereas the supraoccipital (Su), exoccipital (Ex), frontal (Fr) and squamosal (Sq) bones were present but hypoplastic (G). (I and J) The lack of the parietal and interparietal bones was confirmed by micro-CT analyses of living newborn *Tgfbr2*^{Prx1KO} mice, indicating that it was not caused by the accidental removal of the vault during the Alizarin red/Alcian blue staining procedure (I).

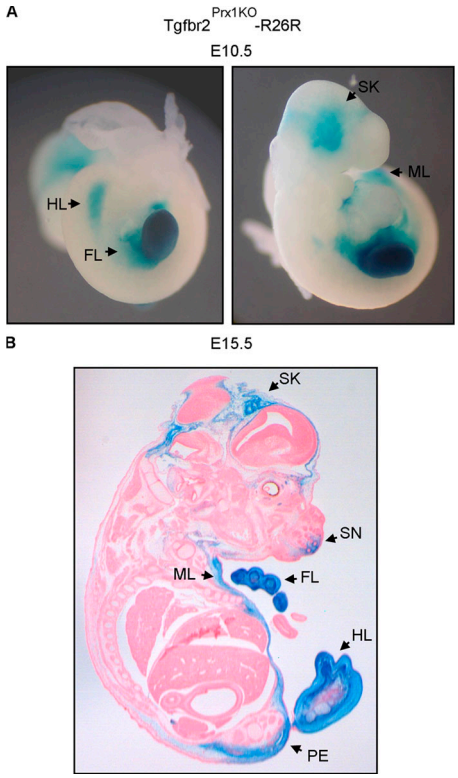

Figure 4. **Expression pattern of Prx-1–mediated Cre recombination in whole mount and sectioned *Tgfbr2*^{Prx1KO}*-R26R* embryos.** (A and B) X-galactosidase staining of a whole mount E10.5 *Tgfbr2*^{Prx1KO}*-R26R* embryo (A) and section of X-galactosidase–stained E15.5 *Tgfbr2*^{Prx1KO}*-R26R* embryo (B). Histological sections were lightly counterstained with Nuclear Fast red. In the E10.5 mutant embryo, the X-galactosidase blue staining, indicating a Cre-catalyzed recombination event, is visible through the forelimb (FL) and hindlimb (HL) buds, skull (SK), and anterior midline region (ML). In the E15.5 mutant embryo, Cre activity is additionally present in the pelvis (PE) and snout (SN) region (regions are marked by arrows). The expression pattern of PRX-1–mediated Cre recombination closely matches the regions where the *Tgfbr2*^{Prx1KO} mutant presents substantial skeletal abnormalities.

so that Cre recombination results in *LacZ* expression (Soriano, 1999). We found that in *Tgfbr2*^{Prx1KO}-R26R whole mount embryos (E10.5), X-galactosidase staining was evident in the developing forelimbs and hindlimbs as well as in the skull and in the anterior midline region of the trunk (Fig. 4 A). In sections of E15.5 *Tgfbr2*^{Prx1KO}-R26R embryos, X-galactosidase staining was visualized in the skull, limbs, and in the oral, midline, and pelvic regions, which are areas where the *Tgfbr2*^{Prx1KO} newborn mutants showed substantial skeletal abnormalities (Fig. 4 B).

TβRII is highly and specifically expressed in developing joints

Because the *Tgfbr2*^{Prx1KO} autopods lacked the interphalangeal joints, we decided to investigate the TβRII expression in developing joints. To this purpose, we modified bacterial artificial chromosomes (BACs) to generate a *Tgfbr2-GFP-β–GEO-BAC* mouse reporter transgene containing both GFP and IRES-β-GEO (LacZ/Neo) reporter genes. We found that in E12.5 (Fig. 5 A, arrows) and 16.5 (Fig. 5 B) whole mount and E16.5 phalangeal sections (Fig. 5 C) of *Tgfbr2-GFP-β–GEO-BAC* embryos, *Tgfbr2* is highly expressed in the interphalangeal joints. We have also noted that *Tgfbr2* is highly expressed in the shoulder and elbow joints (Fig. 5 B) as well as in the knee and hip joints (not depicted). We have established five independent transgenic *Tgfbr2-GFP-β–GEO-BAC* lines that demonstrate *Tgfbr2* joint expression. *Tgfbr2* expression was similar in hindlimb and forelimb interphalangeal joints (unpublished data).

The *Tgfbr2* joint expression pattern in *Tgfbr2-GFP-β–GEO-BAC* mice was directly comparable with endogenous expression. In fact, in situ hybridization studies revealed that in E16.5 *Tgfbr2*$^{flox/flox}$ embryos, *Tgfbr2* is highly expressed in the cells demarking the interphalangeal joint interzone and in the phalangeal prehypertrophic chondrocytes (Fig. 5 D, middle). Immunofluorescence studies confirmed TβRII joint expression (Fig. 5 D, top). Furthermore, there was an intense staining of phosphorylated Smad-2 in the interzone cell nuclei (Fig. 5 D, bottom). In *Tgfbr2*^{Prx1KO} mutants, the lack of joints was accompanied by

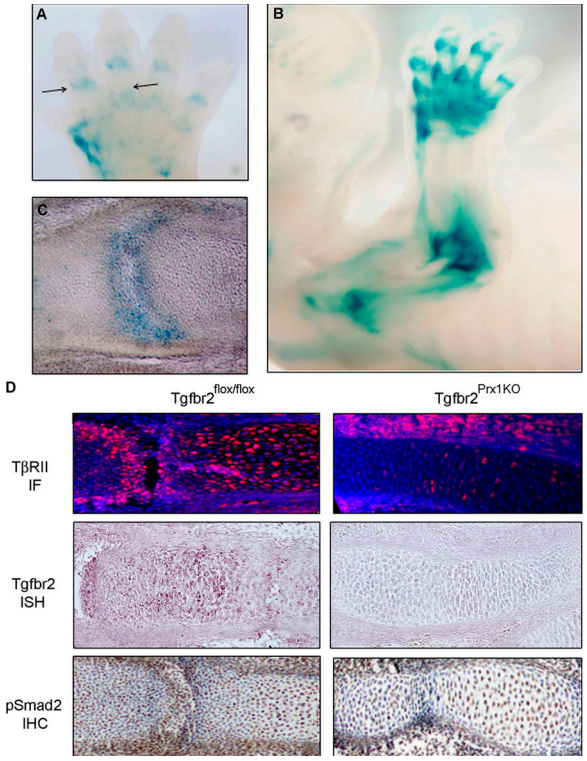

Figure 5. **In the developing interphalangeal joint interzone, the TβRII is highly and specifically expressed, and the R-Smad signaling is activated.** (A–C) E12.5 (A) and E16.5 (B and C) *Tgfbr2-GFP-β−GEO-BAC* forelimbs were subjected to X-galactosidase staining. Intense staining is present in the proximal and medial interphalangeal joints (A and B) as well as in the elbow and shoulder joints (B). (C) Cryosection of an E16.5 forelimb medial interphalangeal joint confirmed intense staining. (D) Paraffin sections of an E16.5 medial interphalangeal joint from the $Tgfbr2^{flox/flox}$ control and $Tgfbr2^{Prx1KO}$ mutant were subjected to TβRII immunofluorescence (IF; top), *Tgfbr2* in situ hybridization (ISH; middle), and immunohistochemistry for phosphorylated Smad-2 (IHC; bottom). Immunofluorescence for TβRII was visualized by Cy3 fluorescence (red), and nuclei were counterstained with Hoechst 33258 (blue). In $Tgfbr2^{flox/flox}$, *Tgfbr2* was expressed in the joint cells and in the phalangeal prehypertrophic chondrocytes. The $Tgfbr2^{Prx1KO}$ mutants lacked *Tgfbr2* expression in the joints and chondrocytes. Nuclear immunostaining for phosphorylated Smad-2 was visualized in brown, and sections were counterstained using hematoxylin. Nuclei of joint cells from $Tgfbr2^{flox/flox}$ mice showed an intense phosphorylated Smad-2 staining that was abrogated in $Tgfbr2^{Prx1KO}$ mutant joints and largely in the phalangeal chondrocytes, providing evidence that TβRII signaling is activated in normal joints but abrogated in mutants. Studies were performed in at least two sections for each antibody and six sections for the *Tgfbr2* probe; sections were obtained from at least two mutant and control embryos.

the lack of *Tgfbr2* mRNA and protein expression as well as a decrease of cell nuclei positive for phosphorylated Smad-2, indicating the effective Prx-1–mediated Cre recombination of *Tgfbr2* (Fig. 5 D). Regarding the *Tgfbr2* expression in the growth plate adjacent to the joints, we found that it was expressed at a much lower level than joints by cells that morphologically resemble prehypertrophic chondrocytes (Fig. 5 D). PCR amplification of genomic DNA extracted by laser capture microdissection (LCM) from paraffin sections of E16.5 joint cells and cells outlining the joint mesoderm demonstrated a specific *Tgfbr2* recombination and subsequent loss of the floxed alleles (*Tgfbr2* exon 2) in $Tgfbr2^{Prx1KO}$ joints compared with $Tgfbr2^{flox/flox}$ (Fig. S1, available at http://www.jcb.org/cgi/content/full/jcb.200611031/DC1). Furthermore, quantitative real-time PCR of genomic DNA extracted from $Tgfbr2^{Prx1KO}$ and $Tgfbr2^{flox/flox}$ forelimb- and hindlimb-dissected digit bones and interphalangeal joints after removal of the skin and surrounding tissues showed that the efficiency of deletion of the *Tgfbr2* exon 2 was 92 ± 3.0% (n = 3 mice for each group); considering the heterogeneity of the sample, efficiency is considerable.

TGF-β signaling initiates joint interzone formation, determining chondrocyte segmentation and interzone cell survival

Initiation of the joint interzone is demarked by segmentation of the cartilaginous continuity across the future joint location (for review see Archer et al., 2003). In $Tgfbr2^{Prx1KO}$ mutants at E16.5, we found a persistence of *Collagen 2*–expressing chondrocytes along the whole digit, including the potential joint site, whereas in control animals at the same age, *Collagen 2* expression was confined to the endochondral templates and absent in the fully demarked joint (Fig. 6 A). Several components of the Notch system are expressed in articular cartilage, and a Notch-1–positive population of progenitor joint cells has been recently isolated from articular cartilage. This leads to the hypothesis that Notch signaling within the articular cartilage blocks chondrocyte differentiation, maintaining clonality and proliferation of the progenitor joint-forming cells (Hayes et al., 2003; Dowthwaite et al., 2004). In mice, interzone develops at E12.5–13.5. We found that E13.5 $Tgfbr2^{Prx1KO}$ mutants failed to form the interzone and lacked Jagged-1 expression, whereas in control mice, interzone cells highly expressed Jagged-1 (Fig. 6 B). It has been postulated that apoptosis may play a role in determining the fate of differentiated chondrocytes within the developing joint (for review see Archer et al., 2003). An intense positive TUNEL staining for apoptotic nuclei was observed in E13.5 control forming joints, whereas $Tgfbr2^{Prx1KO}$ E13.5 mutants lacked cell apoptosis within the presumptive joint region (Fig. 6 C).

TGF-β signaling is required for joint morphogenic gene expression

The activation of *Noggin* transcription is critical for joint formation, although its regulation is unknown. Mice that are null mutants for *Noggin* lack joints, and *Noggin* heterozygous loss of function mutations are found in some of the patients with proximal symphalangism (SYM1-OMIM185800) that lack proximal and medial interphalangeal joints, whereas the distal interphalangeal joint is never affected (Brunet et al., 1998; Gong et al., 1999; Takahashi et al., 2001). Analysis of *Noggin* expression at E13.5 and 16.5 by in situ hybridization and immunofluorescence revealed a complete down-regulation in the joints of $Tgfbr2^{Prx1KO}$ embryos (Fig. 7, A and B). *Gdf-5* is one of the earliest markers expressed in developing joints, and *Gdf-5* is mutated in the *brachypodism* mouse, which has interphalangeal joint defects (Storm et al., 1994). Furthermore, a *Gdf-5* mutation with a gain of aberrant BMP-2–like function was reported in a family with SYM1 (Seemann et al., 2005). It has been hypothesized that in early chondrogenesis, *Gdf-5* inhibits joint formation and induces cartilage development, whereas its role in late chondrogenesis

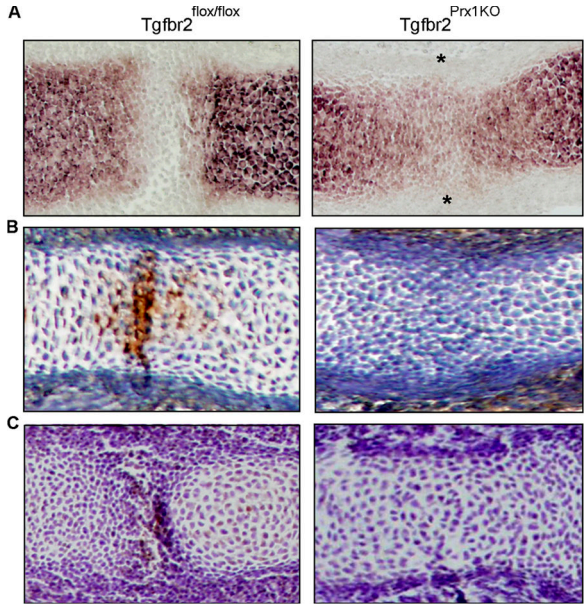

Figure 6. **TGF-β signaling is needed for chondrocyte segmentation and interzone cell apoptosis.** (A) Paraffin sections of an E16.5 hindlimb medial interphalangeal joint from the *Tgfbr2*^{Prx1KO} mutant and *Tgfbr2*$^{flox/flox}$ control were subjected to in situ hybridization for *Collagen 2*. In *Tgfbr2*^{Prx1KO} mutants, at the site where the presumptive joints should have formed, a persistence of *Collagen 2* expression was found, as indicated by asterisks. (B) Paraffin sections of an E13.5 medial interphalangeal joint from the *Tgfbr2*^{Prx1KO} mutant and *Tgfbr2*$^{flox/flox}$ control were subjected to immunohistochemistry analyses for Jagged-1 expression. The sections were lightly counterstained with hematoxylin. In control embryos, an intense Jagged-1 expression was detected in the interzone cells, whereas mutants lacked any detectable Jagged-1 in the presumptive joints. The increased cell density noted at the presumptive joint sites of the mutant is a sporadic finding most likely caused by a technical problem during the sectioning process. (C) Paraffin sections of an E13.5 medial interphalangeal joint from the *Tgfbr2*^{Prx1KO} mutant and *Tgfbr2*$^{flox/flox}$ control were subjected to TUNEL assay, and fragmented DNA of apoptotic cells were visualized as brown nuclei. The sections were lightly counterstained with hematoxylin. In control embryos, an intense staining of apoptotic nuclei was visualized in the interzone, *Tgfbr2*^{Prx1KO} mutants lacked the interzone, and no sign of apoptosis was detected in the presumptive joint. Studies were performed in at least two sections for Jagged-1 antibody and TUNEL assay and at least six sections for the Collagen 2 probe; sections were obtained from at least two mutant and control embryos.

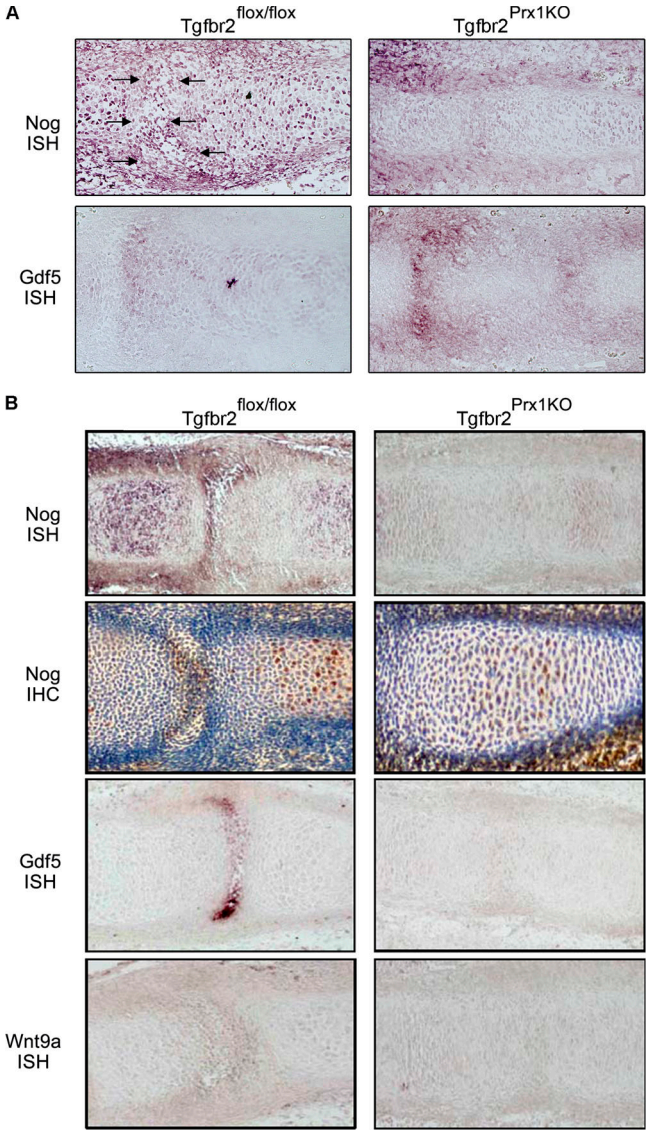

Figure 7. **TGF-β signaling is essential for *Noggin*, *Gdf-5*, and *Wnt9a* expression in the interphalangeal joints.** (A and B) Paraffin sections of an E13.5 (A) and E16.5 (B) hindlimb medial interphalangeal joint from the *Tgfbr2*^{Prx1KO} mutant and *Tgfbr2*$^{flox/flox}$ control were subjected to in situ hybridization (ISH) for *Noggin* (Nog; A and B, top), immunohistochemistry (IHC) for Noggin (B, second row), in situ hybridization for *Gdf-5* (B, third row), and *Wnt9a* (B, fourth row). *Tgfbr2*^{Prx1KO} mutants showed a down-regulation of *Noggin* at E13.5 and E14.5; *Gdf-5* was up-regulated at E13.5, whereas it was down-regulated at E16.5; Wnt9a was down-regulated at E16.5. Arrows indicate the control developing interzone joint. Studies were performed in at least two sections for Noggin antibody and at least six sections for the Noggin, Gdf-5, and Wnt9a probes; sections were obtained from at least two mutant and control embryos.

is to maintain joint formation (Storm and Kingsley, 1999). In *Tgfbr2*^{Prx1KO} mutants, *Gdf-5* expression was increased at E13.5, whereas it was abrogated in E16.5 (Fig. 7, A and B). *Wnt9a* is expressed in developing joints, and its misexpression in chicken digit rays induces ectopic joint formation, whereas the loss of *Wnt9a* in mice results in synovial chondromatosis (Hartmann and Tabin, 2001; Spater et al., 2006). In *Tgfbr2*^{Prx1KO} mutant joints, *Wnt9a* expression is down-regulated in E13.5 (not depicted) and 16.5 (Fig. 7 B). These results indicate that TGF-β signaling in developing limbs is mandatory for joint formation and to regulate *Noggin*, *Gdf-5*, and *Wnt9a* expressions.

TGF-β signaling regulates Noggin expression and BMP activity in limb bud micromass cultures

It is difficult to infer from the results found in *Tgfbr2*^{Prx1KO} mutants whether TGF-β signaling directly regulates *Noggin* transcription or whether TGF-β sustains the limb bud growth, ensuring an adequate environment for the joints to develop and *Noggin* to be expressed. Therefore, we decided to evaluate the role of TGF-β signaling in *Noggin* expression in limb bud micromass cultures. In *Cre*$^{+}$*Tgfbr2*^{KO} cultures, *Tgfbr2* expression was conditionally inactivated, and the lack of TβRII binding expression was verified by a ^{125}I–TGF-β1 affinity cross-linking cell surface–binding assay (Fig. S2 A, available at http://www.jcb.org/cgi/content/full/jcb.200611031/DC1). In control

MMP⁺Tgfbr2$^{flox/flox}$ cultures, the TβRI, TβRII, and TβRIII were identified, whereas in *Cre⁺Tgfbr2^{KO}* cultures, ^{125}I–TGF-β1 binding to TβRII was greatly reduced (Fig. S2 A). The specificity of ^{125}I–TGF-β1 binding was confirmed by the fact that labeled bands were displaced by cold TGF-β1 in excess (Fig. S2 A). Cre recombination was also confirmed by an intensely positive X-galactosidase staining in *Cre⁺Tgfbr2^{KO}-R26R* that was negative in control *MMP⁺Tgfbr2$^{flox/flox}$-R26R* cultures (Fig. S2 B).

We found that in *MMP⁺Tgfbr2$^{flox/flox}$* cultures, TGF-β treatment induced Noggin mRNA and protein expression as determined by quantitative RT-PCR and Western immunoblotting (WIB) analyses (Fig. 8, A and B). Similar results were found when wild-type micromass cultures were treated with TGF-β (7.8 ± 2.1-fold compared with untreated control [1.2 ± 0.3-fold]; $P < 0.05$; $n = 3$). Noggin binds to BMPs, preventing BMP receptor activation and, therefore, signaling; the canonical BMP signal is through the phosphorylation cascade of Smad-1, -5, and -8 that complex and induce transcription. Therefore, in accordance with the increase of *Noggin* expression, we found that in *MMP⁺Tgfbr2$^{flox/flox}$* cultures, TGF-β decreased BMP activity, as indicated by a decrease of phosphorylated Smad-1, -5, and -8 (Fig. 8 B). Knocking out the TGF-β signaling in *Cre⁺Tgfbr2^{KO}* cultures resulted in the abrogation of TGF-β effects on Noggin expression and Smad-1, -5, and -8 phosphorylation (Fig. 8, A and B). Notably, a decrease of Smad-1, -5, and -8 phosphorylation was found in untreated *Cre⁺Tgfbr2^{KO}* compared with *MMP⁺Tgfbr2$^{flox/flox}$* cultures, possibly as a result of the unresponsiveness of *Cre⁺Tgfbr2^{KO}* cells to endogenous TGF-β.

TGF-β signaling in autopod endochondral cartilage development

It has been hypothesized that the developing joints act as signaling centers to control the adjacent endochondral template development (for review see Archer et al., 2003). Because the *Tgfbr2^{Prx1KO}* mutant lacks the interphalangeal joints, it represents an ideal model to test this hypothesis. Therefore, we performed a systematic evaluation of cartilage marker expressions in growth plates adjacent to the presumptive interphalangeal joints at E13.5, E16.5, and postnatal day (P) 0 in *Tgfbr2^{Prx1KO}* mutants and control *Tgfbr2$^{flox/flox}$* siblings (Fig. 9, A–C). We found that *Tgfbr2^{Prx1KO}* growth plates presented several remarkable and selective abnormalities; *Collagen 10* expression is consistently decreased at E13.5, E16.5, and P0 compared with Tgfbr2$^{flox/flox}$ controls, indicating a dramatic delay in chondrocyte hypertrophy in the mutants (Fig. 9, A–C). Conversely, in *Tgfbr2^{Prx1KO}* growth plates, *Indian hedgehog* (*Ihh*) was increased and more widely expressed from the proliferative zone to the canonical prehypertrophic chondrocyte zone compared with Tgfbr2$^{flox/flox}$ controls; this finding was consistent at E13.5, E16.5, and P0 (Fig. 9, A–C). In *Tgfbr2^{Prx1KO}* mutants at E16.5 and P0, parathyroid hormone–related protein (*PTH-rP*) expression is increased and more diffuse in the prehypertrophic/upper proliferative zone and in the perichondrium; at E13.5, *PTH-rP* expression is similar to the control (Fig. 9, A–C). *Collagen 2* and *Sox-9* expressions are similar to the control in *Tgfbr2^{Prx1KO}*, but *Collagen 2*–expressing cells at P0 display a less organized columnar distribution than controls (Fig. 9, A–C). This disorganization was also observed in the hematoxylin and eosin staining that also showed that hypertrophic chondrocytes are larger but show a decreased expression of *Collagen 10* (Fig. 9 C).

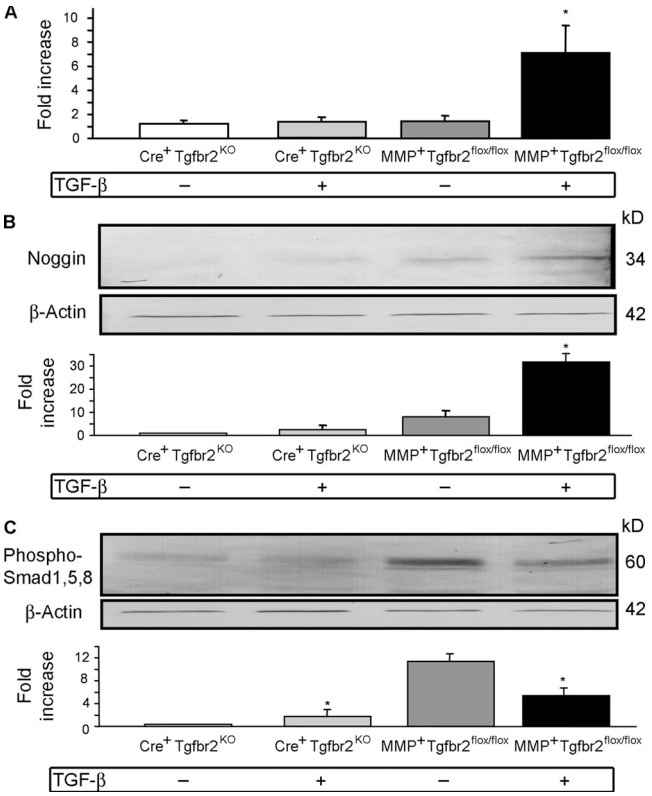

Figure 8. **TGF-β signaling up-regulates Noggin and down-regulates BMP activity.** (A–C) Micromass cultures of mesenchymal limb bud cells were obtained from E11.5 *Tgfbr2$^{flox/flox}$* mice. To knockout *Tgfbr2*, cultures were retrovirally infected either with the HR-MMPCreGFP vector (Cre recombinase) to generate Cre⁺Tgfbr2^{KO} micromasses or with MMP-GFP empty vector to generate MMP⁺Tgfbr2$^{flox/flox}$ micromasses. mRNA and cell lysates were obtained from cultures treated with or without 20 ng/ml TGF-β for 36 h and were subjected to quantitative RT-PCR (A) or WIB (B) for Noggin expression or WIB (C) for phosphorylated Smad-1, -5, and -8. *Noggin* expression was normalized to *glyceraldehyde-3-phosphate dehydrogenase* expression and expressed as fold of increases compared with the lowest value found in the untreated control, which was given an arbitrary value of 1. TGF-β induced Noggin mRNA and protein expressions, and the effect was abrogated in Cre⁺Tgfbr2^{KO} micromasses. In accordance with the increase of Noggin expression, we found that in MMP⁺Tgfbr2$^{flox/flox}$ cultures, TGF-β induced a down-regulation of BMP activity as documented by a decrease of Smad-1, -5, and -8 phosphorylations; consistently, TGF-β action was abolished in Cre⁺Tgfbr2^{KO} micromasses. Membranes were probed with anti–β-actin antibody as an internal control for the protein amount loaded. For WIB densitometric analysis, band intensity was quantified, and background intensity was subtracted and normalized by the respective β-actin band intensity. Plots are represented, and mean ± SD (error bars) as the fold increase over control is given. *, $P < 0.05$ versus untreated MMP⁺Tgfr2$^{flox/flox}$ by one-way analysis of variance; $n = 3$.

Discussion

The role of TGF-β signaling in skeletogenesis is not well determined, and contradictory data have been reported (for review see Dunker and Krieglstein, 2000). We have generated the *Tgfbr2^{Prx1KO}* mutant mice in which the *Tgfbr2* is conditionally inactivated in limb buds and a subset of mesenchyme tissues starting at very early embryonic limb development. The *Tgfbr2^{Prx1KO}*

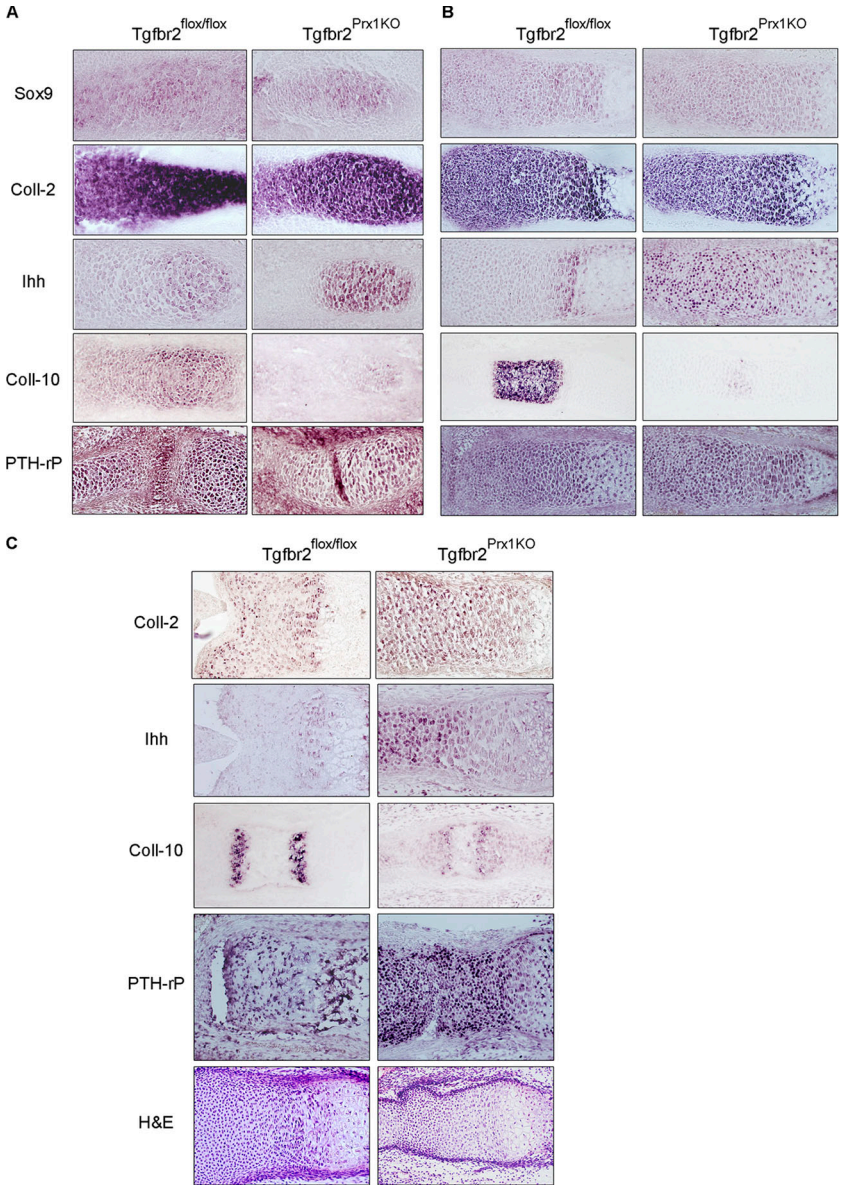

Figure 9. **TGF-β signaling in cartilage development: lack of joint development is associated with selective effects on the adjacent chondrogenesis.** (A–C) Paraffin sections of E13.5 (A), E16.5 (B), and P0 (C) growth plates adjacent to the (presumptive) interphalangeal joint of the *Tgfbr2*^{Prx1KO} mutant and *Tgfbr2*$^{flox/flox}$ control were subjected to in situ hybridization for *Sox-9* (A and B, top), *Collagen 2* (A and B, second rows; and C, top), *Ihh* (A and B, third rows; and C, second row), *Collagen 10* (A and B, fourth rows; and C, third row), *PTH-rP* (A and B, bottom; and C, fourth row), or hematoxylin and eosin staining (C, bottom). *Tgfbr2*^{Prx1KO} mutants showed an up-regulation of *Ihh* and a down-regulation of *Collagen 10* expressions at all stages. *Collagen 2* and *Sox-9* expressions were similar in *Tgfbr2*^{Prx1KO} and control, but *Collagen 2*–expressing cells at P0 display a less organized columnar distribution than controls. *PTH-rP* expression in E13.5 *Tgfbr2*^{Prx1KO} mutants is similar to the control, whereas at E16.5 and P0, it is increased in the perichondrium and especially in the prehypertrophic/upper proliferative cells. Studies were performed in at least six sections for each probe that were obtained from at least two mutant and control embryos.

mouse allowed us to determine that TGF-β signaling is essential for interphalangeal joint development. TGF-β signaling initiates the joint interzone formation by regulating interzone cell survival and chondrocyte segmentation. TGF-β elicits these effects operating upstream of Noggin, GDF-5, and Wnt9a expressions. Our results uncover a novel step regulated by TGF-β signaling that is required for establishing the correct initiation of joint development.

TβRII and signaling are expressed in the limb joints

Although a role of TGF-β signaling in joints has been speculated, TβRII expression in joints has never been clearly reported. To incontrovertibly define that TβRII is expressed in developing interphalangeal joints, we generated the *Tgfbr2-GFP-β−GEO-BAC* mouse reporter transgene and used immunofluorescence and in situ hybridization studies. Furthermore, we found a high staining of phosphorylated Smad-2 in the interzone cell nuclei, corroborating the finding that TβRII is expressed in the cells, demarking the interzone and signaling through the R-Smad pathway. The Tgfbr2-GFP-β−GEO-BAC mouse allowed us to observe that *Tgfbr2* is also highly expressed in the proximal limb joints. The Tgfbr2^{Prx1KO} mutants lack only the interphalangeal joints, whereas the proximal limb joints are formed. It may be possible that the Prx-1–mediated Cre recombination expression varies within the limb and is present in the interphalangeal joints, whereas it is lacking or less effective in the proximal limb joints. Another possibility is that TGF-β signaling is essential for interphalangeal joint development, whereas it is dispensable for development of the proximal limb joints. The efficiency and specificity of the Prx-1–mediated Cre recombination of TβRII in the joints was supported by the in situ hybridization and immunofluorescence studies and by the PCR amplification analyses of joint cell DNA obtained by LCM of joint cells or from digit bones and interphalangeal joints.

TGF-β signaling is essential for interzone formation

Joints in *Tgfbr2*^{Prx1KO} mutants appear to be arrested in their development at about the time at which interzone starts to develop: differentiated chondrocytes extend with a continuous pattern across the phalanges without any sign of apoptosis, and interzone cells lack Jagged-1 expression and any sign of condensation. The molecular mechanisms underlying interzone formation are not yet well understood. Although Wnt9a was reported as a potential joint inducer, the recent report that Wnt9a-null mice have joints has redefined its role more as a joint keeper (Hartmann and Tabin, 2001; Spater et al., 2006). GDF-5 is highly expressed in developing joints. It has been hypothesized that in early chondrogenesis (E14.5), *Gdf-5* inhibits joint formation and induces cartilage development, whereas at a later stage of chondrogenesis (E15.5), it regulates joint structure formation or maintenance (Storm and Kingsley, 1999). Our data indicate that TGF-β signaling down-regulates joint GDF-5 expression at an early chondrogenesis stage, whereas it up-regulates its joint expression at a later stage, suggesting that it operates upstream of GDF-5.

Another conundrum in understanding joint interzone development is the fate of differentiated chondrocytes and in the meantime emergence of the interzone cells. It has been recently reported that a distinct mesenchymal cell population takes part in the interzone and articular layer formation (Pacifici et al., 2006). Furthermore, a Notch-1–positive progenitor cell population has been recently isolated within the articular cells. These Notch-1 progenitors are capable of engrafting in vivo into articular structures and have been hypothesized to maintain articular cartilage integrity, preserving interzone cell clonality and proliferation while preventing differentiation into chondrocytes (Dowthwaite et al., 2004). To corroborate this hypothesis, a derangement of the Notch signaling has been reported in articular synoviocytes from patients with rheumatoid arthritis that is characterized by aberrant synoviocyte proliferation (Ando et al., 2003). A direct cross talk between the Notch and TGF-β signaling pathways comes from a recent study in which a direct interaction between Notch intracellular domain and Smad-3 was demonstrated, and activation of Smad-3 by TGF-β led to an enhancement of Notch-induced Hes1 gene transcription (Blokzijl et al., 2003). We hypothesize that TGF-β serves as an essential joint signaling center and that activating Notch signaling forces progenitor interzone cells to remain in an undifferentiated state while regulating the apoptosis of differentiated chondrocytes. Our hypothesis needs further investigation, and the possibility that down-regulation of Jagged-1 in the *Tgfbr2*^{Prx1KO} mutants is consequent to the lack of interzone formation should also be considered. In bone marrow–derived mesenchymal stem cells, we have previously reported that TGF-β induces chondrogenesis by exerting similar dichotomic effects (Longobardi et al., 2006). Deciphering the role of TGF-β signaling in joint development can provide substantial insight to identify the interzone cells and to define the role of chondrocyte-programmed cell death and progenitor interzone cell survival in joint formation.

The TGF-β ligand expression pattern in developing cartilage has been previously reported, including by our group (Pelton et al., 1991a,b; Lawler et al., 1994). TGF-β1 is expressed in the digit perichondrium at E13.5, and, by E16.5, TGF-β2 and -β3 are also expressed in the perichondrium, including in the digit perichondrium (Millan et al., 1991; Pelton et al., 1991a,b; Lawler et al., 1994; Serra and Chang, 2003). It has been previously reported that in cartilage development, TGF-βs exert their actions in a paracrine fashion (Lawler et al., 1994). We hypothesize that a similar mechanism occurs during digit joint development. Future studies are needed to evaluate TGF-β ligand delivery to the interphalangeal joints.

TβRII operates upstream of joint gene expression, induces Noggin expression, and modulates BMP activities in vitro

Our data indicate that TGF-β signaling in the joints functions as a master regulator for expression of the key joint morphogenic genes *GDF-5*, *Noggin*, and *Wnt9a*. We propose a working hypothesis model for joint development in which TGF-β signaling is essential in inducing the joint interzone formation, and it operates early in joint development to regulate the expression of critical joint morphogenic genes such as *Noggin* to modulate BMP activities (Fig. 10).

The joint phenotype observed in the *Tgfbr2*^{Prx1KO} mouse is similar to that in patients with proximal symphalangism (SYM1-OMIM185800) in which the proximal and medial interphalangeal joints are lacking, whereas the distal interphalangeal joint is not affected (Gong et al., 1999; Takahashi et al., 2001). Although functionally the distal interphalangeal joint is indistinguishable from the other interphalangeal joints, the observation of phenotypical abnormalities only affecting the proximal and medial interphalangeal joints in patients with SYM1 and now in the *Tgfbr2*^{Prx1KO} mouse indicates a distinct development for the distal joint. In patients with SYM1, heterozygous mutations of Noggin as well as a heterozygous mutation of GDF-5 with an aberrant BMP-like gain of function have been reported (Gong et al., 1999; Seemann et al., 2005). Furthermore, Noggin-null mutant mice lack joint development (Brunet et al., 1998). These findings clearly indicate that lack of Noggin function or increase in BMP activities result in the failure of joint development. The regulatory factors that determine Noggin expression within the joints are unknown. Our data indicate that *Noggin* expression is down-regulated in the *Tgfbr2*^{Prx1KO} mouse, and, in limb bud cultures, TGF-β induces *Noggin* expression and reduces BMP signaling. Gazzerro et al. (1998) have previously reported that TGF-β1 induces *Noggin* mRNA in cultured rat osteoblasts with unclear function. Our working hypothesis is that TGF-β signaling induces joint development by regulating Noggin expression and, therefore, BMP activities. However, considering the multiple and diverse limb abnormalities found in the *Tgfbr2*^{Prx1KO} phenotype, it seems likely that more than one mechanism would be involved. We have noted that in E13.5 mutants compared with controls, *Noggin* mRNA was increased in the surrounding tissue but was not increased at E16.5; on the other hand, at E16.5, we noted an increase of protein expression. We hypothesize that at E13.5, the lack of *Noggin* joint expression leads to a compensatory response in the surrounding tissue that is associated with an increase of protein expression still detectable at

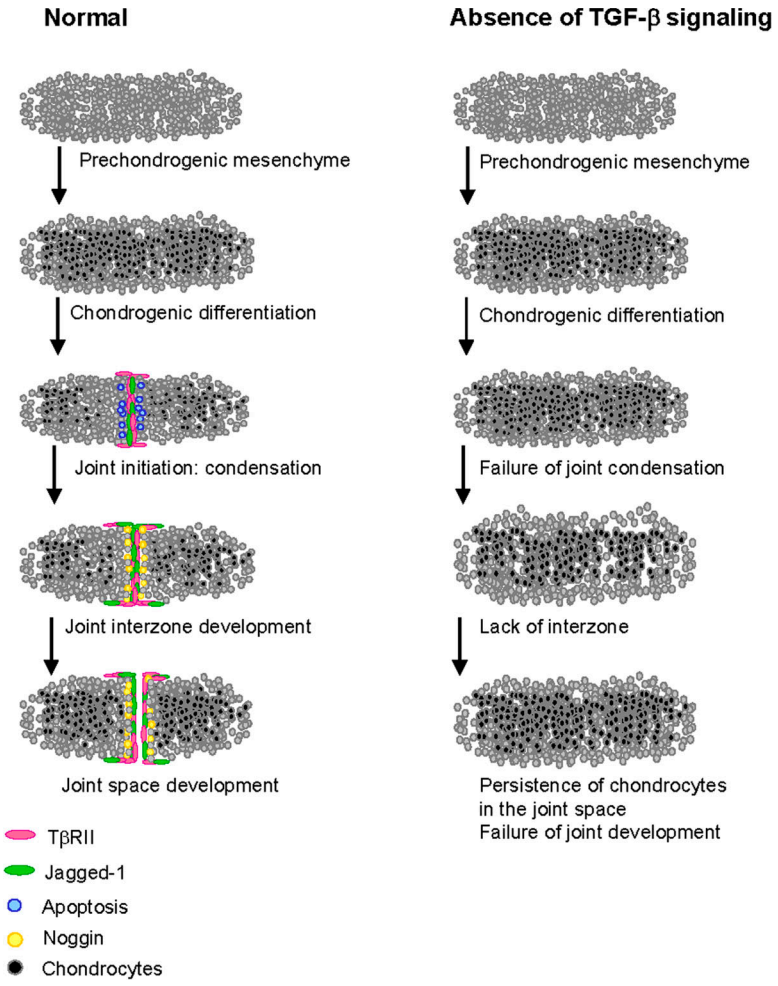

Figure 10. **TGF-β is a master signaling center within the joint interzone.** Proposed model for the role of TβRII signaling in interphalangeal joint development. TβRII is specifically expressed by the joint-developing cells, and lack of TGF-β signaling results in the failure of interzone formation by lack of the survival of interzone-forming cells, persistence of differentiated chondrocytes in the joint region, and derangement of joint morphogenic gene expressions.

E16.5 (probably as a result of a prolonged protein half-life). However, at E16.5, this mRNA compensatory response seems to be defective. Future studies are needed to identify the mechanisms responsible for this compensatory response. In the controls, *Noggin* expression in the surrounding tissue is greater at E16.5 than at 13.5; the significance of this increase is also unclear, and further studies outside of the scope of the present experiments are needed to determine this.

TGF-β signaling in cartilage development: lack of joint development is associated with selective effects on the adjacent chondrogenesis

We have found that in *Tgfbr2*^{Prx1KO} mutants, the growth plates adjacent to the interphalangeal joints present an increase of *Ihh* expression and a decrease of *Collagen 10* expression at early as well as late chondrogenesis; *PTH-rP* expression is increased in late chondrogenesis. GDF-5–releasing beads implanted in the interdigital space of developing mouse limbs resulted in an increase of *Ihh* expression that has also been noted in *Noggin*-null mutant mice. Up-regulation of Ihh signaling in *Patched-1*$^{-/-}$*; Collagen 2a1-Cre* mice resulted in joint fusion (Brunet et al., 1998; Storm and Kingsley, 1999; Mak et al., 2006). We hypothesize that TGF-β signaling within the joints plays a central role in orchestrating the interplay between joint formation and adjacent endochondral template development by controlling *Ihh* expression that induces *PTH-rP* and, thus, repressing the rate of chondrocyte hypertrophy. Interestingly, in *Tgfbr2*^{Prx1KO} mutants, *PTH-rP* expression is increased in the perichondrium but more remarkably in the prehypertrophic/upper proliferative cells. Using a PTH-rP–LacZ reporter mouse, Chen et al. (2006) have recently reported that PTH-rP is expressed in this subpopulation of cells. The role of these PTH-rP–expressing cells is still not clearly defined, but they may contribute to the PTH-rP inhibitory effect on hypertrophy (Chen et al., 2006). Hematoxylin and eosin morphometric analysis showed that hypertrophic chondrocytes seem to be larger in P0 Tgfbr2$^{PRX-1KO}$ mutants, but Collagen 10 expression was clearly decreased at any stage, indicating a functional derangement. These findings are consistent with our hypothesis that TGF-β signaling is required for the appropriate progression of the prehypertrophic to hypertrophic chondrocytes, and its abolishment is associated with a derangement of the pre- and hypertrophic growth plate zones.

Our data are only apparently in contradiction with the findings observed in *Tgfbr2*$^{flox/flox}$*Collagen 2a-cre* mice in which *Tgfbr2* was conditionally inactivated in Collagen 2a–expressing cells. In the *Tgfbr2*$^{flox/flox}$ *Collagen 2a-cre* mouse, chondrocyte differentiation and development of long bones are normal. We hypothesize

that in the endochondral growth process, TGF-β signaling is required to control the rate of differentiation of prehypertrophic chondrocytes to hypertrophic chondrocytes, whereas it has relatively scarce effect on collagen 2–expressing chondrocytes. An increase of *Ihh* expression was found in the growth plates of newborn DNIIR, and, by 1–2 mo of age, these mice develop progressive osteoarthritis with replacement of the articular cartilage with Collagen X– expressing cells (Serra et al., 1997). We speculate that over time, DNIIR mice develop a compensatory mechanism that overrides the Ihh inhibitory effect on hypertrophy.

TGF-β signaling regulates calvaria development

The *Tgfbr2*^{Prx1KO} mouse lacks the parietal and interparietal bones. Interestingly, a similar phenotype has been reported in patients with familial parietal foramina (PFM-1, OMIM168500 PFM-2, and OMIM609597) that have symmetrical, oval defects in the parietal bones. Some of these patients have been reported to have haploinsufficiency either in the homeobox gene *Alx4* (OMIM609597) or in the *Msx2* gene (OMIM168500; Wuyts et al., 2000a,b) In mice, *Msx2*, *Twist*, and *Alx4* cooperate in controlling the migration and differentiation of crest-derived skeletogenic mesenchyme in the vault (Ishii et al., 2003; Antonopoulou et al., 2004). Cranio-facial conditional inactivation of *Tgfbr2* in the *Tgfbr2*$^{flox/flox}$*;Wnt1-cre* mouse also resulted in calvaria defects (Ito et al., 2003). We have noted that in the *Tgfbr2*^{Prx1KO}-R26R mouse, the LacZ-stained cells are arrested below the parietal and interparietal bones (Fig. 5, A and B), whereas in controls, LacZ-stained cells cover the vault (not depicted). The flat bones of the skull vault develop from two migratory mesenchymal cell populations, the cranial neural crest, and paraxial mesoderm. The possibility that a defect in migration of the *Tgfbr2*^{Prx1KO} skeletogenic mesenchyme cells within the vault can lead to the vault bones and the interplay between TGF-β signaling with *Msx2*, *Twist*, and *Alx4* genes is under investigation, and further studies are needed. In conclusion, the *Tgfbr2*^{Prx1KO} mouse model has unraveled critical information on skeletal development and opened novel potential therapeutic approaches to treat degenerative joint diseases such as osteoarthritis.

Materials and methods

Generation of Tgfbr2^{Prx1KO}, Tgfbr2-GFP-β−GEO-BAC, and Tgfbr2^{Prx1KO}-R26R mice

To generate *Tgfbr2*^{Prx1KO} mutants, female *Tgfbr2*$^{flox/flox}$ homozygous mice were mated with *Prx1-Cre* and *Tgfbr2*^{flox} heterozygous males (Chytil et al., 2002; Logan et al., 2002). As previously reported, we have generated the *Tgfbr2*$^{flox/flox}$ mouse by flanking with loxP sites the exon 2 of TβRII that transcribes for the TGF-β–binding domain (Chytil et al., 2002). In the *Prx1-Cre* mouse (a gift from C. Tabin, Harvard Medical School, Boston, MA), a *Prx1* limb enhancer drives Cre recombinase expression in limb buds and in calvaria mesenchyme beginning at E9.5 (Logan et al., 2002). Genotyping was performed using PCR primers for *loxP* and *Cre* (Chytil et al., 2002). Because a penetrant germline recombination has been reported when crossing *Prx1-Cre* females with mice carrying floxed genes, only Cre^{+} males were used (Logan et al., 2002). Cre^{+}Tgfbr2$^{flox/-}$ males (Swiss-Webster background) were backcrossed propagated to C57BL/6 *Tgfbr2*$^{flox/flox}$ females, and experiments were performed in mice that were in the C57BL/6 strain for at least eight generations.

To generate the *Tgfbr2-GFP-β−GEO-BAC* mouse, the mouse BAC clone RP24-317C21 containing *Tgfbr2* was obtained from the Children's Hospital Oakland Research Institute. As schematically presented in Fig. S3 (available at http://www.jcb.org/cgi/content/full/jcb.200611031/DC1), a GFP-IRES-β-GEO cassette was inserted into *Tgfbr2-BAC* at the endogenous *Tgfbr2* translational start site using the homologous recombination technique of Warming et al. (2005), Lee et al. (2001), and as previously reported (Mortlock et al., 2003; Deal et al., 2006) as follows: the plasmid pIBGFTet was generated by ligating the IRES-β-GEO-SV40pA cassette from pGT1.8 and an FRT-flanked tetracycline resistance cassette into a modified pBluescript II SK+ backbone (Mountford et al., 1994). An eGFP open reading frame (CLONTECH Laboratories, Inc.) was then inserted upstream of IRES-β-GEO-SV40pA to create pGFPIBGFTet. The recombination cassette was constructed by subcloning 50-bp 5′ and 3′ recombination arms (both containing part of the *Tgfbr2* exon 1) into pGFPIBGFTet such that the recombination arms flanked the GFP-IRES-β-GEO-FRT-Tet-FRT cassette. The forward strand (relative to *Tgfbr2*) sequences of the 50-bp homology arms were as follows: for the 5′ arm, CGGTTCGTGGCGCACCAGGGGCCGGTCTATGACGAGCGACGGGGGCTGCC; and for the 3′ arm, ATGGGTCGGGGGCTGCTCCGGGGCCTGTGGCCGCTGCATATCGTCCTGTG. Both recombination arms were created by annealing PAGE-purified oligonucleotides designed to allow direct ligation to pGFPIBGFTet. The final cassette with recombination arms was digested from the vector, gel purified, and recombined with BAC as described previously (Lee et al., 2001). Successful recombinants were selected by tetracycline resistance. The tetracycline resistance gene was then removed by FLPe recombinase excision (Lee et al., 2001; Mortlock et al., 2003). The correctly modified BAC was verified by conventional and pulsed-field gel analysis of restriction digests to confirm expected banding patterns as well as direct BAC sequencing. *Tgfbr2*-BAC DNA was purified according to established techniques and was used for pronuclear injection of C57BL/6J × DBA/2J F1 hybrid embryos (DiLeone et al., 2000). Injections and oviduct transfers were performed by the Vanderbilt Transgenic Core Facility using standard techniques in accordance with protocols approved by the Vanderbilt University Institutional Animal Care and Use Committee. All BACs were injected as uncut circular DNAs.

To generate the *Tgfbr2*^{Prx1KO}*-R26R* mouse, the *Tgfbr2*$^{flox/flox}$ and *R26R* (obtained from P. Soriano, Fred Hutchinson Cancer Research Center, Seattle, WA; Soriano, 1999) were first crossed to obtain the *Tgfbr2*$^{flox/flox}$*-R26R* female mice that were then crossed with *Prx1-Cre* heterozygous males. For timed pregnancies, noon of the day when evidence of a vaginal plug was found was considered E0.5.

Skeletal analysis

Alizarin red/Alcian blue staining was performed as previously reported (Mortlock et al., 1996). Images were taken using a stereo microscope (SZX16; Olympus) equipped with a digital camera (DP71; Olympus) and imported into Photoshop (Adobe). Living animal micro-CT imaging (Imtek MicroCAT-II-CT) was performed setting micro-CT slices at 40 μm that were then reconstructed in 3D arrays using the same thresholds.

Histology, immunofluorescence, immunohistochemistry, TUNEL assay, in situ hybridization studies, and detection of β-galactosidase activity in whole mount embryos and cryosections

Intact or dissected limb embryos or skinned and decalcified newborns were sectioned using standard procedures. For general morphology, sections were stained with hematoxylin and eosin using standard procedures.

For immunohistochemistry or immunofluorescence, either the CytomationK41010 or VectastatinEliteABC Immunostaining kits (DakoCytomation) were used. The following primary antibodies were used: anti-TβRII polyclonal (Santa Cruz Biotechnology, Inc.), anti–Jagged-1 polyclonal (Santa Cruz Biotechnology, Inc.), antiphosphorylated Smad-2 polyclonal (Cell Signaling), and anti-Noggin polyclonal (R&D Systems). Apoptotic nuclei were visualized using the DeadEnd Colorimetric TUNEL System (Promega).

In situ hybridization studies were performed as previously reported (Deal et al., 2006). Digoxigenin-UTP-riboprobes were synthesized (DIG-RNA-Labeling kit; Roche) from plasmids with insertion of *Noggin* (provided by R. Harland, University of California, Berkeley, Berkeley, CA), *Tbr2* (provided by S.K. Dey, Vanderbilt University, Nashville, TN), mouse *Collagen 2a1* and *Gdf-5* (provided by D. Kingsley, Stanford University, Palo Alto, CA), mouse *Ihh* (provided by A. McMahon, Harvard University, Cambridge, MA), and *PTHrP* (provided by H. Kronenberg, Harvard University; Metsaranta et al., 1991; Storm and Kingsley, 1996; Das et al., 1997). *Wnt9a* was made using a mouse *Wnt9a* cDNA clone (IMAGE clone #30435371; GenBank/EMBL/DDBJ accession no. BC066165); the plasmid

was linearized with XmnI and riboprobe synthesized with T7 polymerase. *Collagen 10a1* and *Sox9* probes were also made. The primers for *Sox9* were forward (GACATGTAAAGGAAGGTAACGATTG) and reverse (AGG CTAAGGGACACTCTTGAACTA); the primers for *Collagen 10a1* were forward (GCCAGGTCTCAATGGTCCTA) and reverse (GATCCAGGTAG-CCTTTGCTG). PCR products were cloned into pGEMT-Easy and linearized with NcoI, and riboprobes were synthesized with T7 polymerase. Whole mount embryo X-galactosidase staining was performed as previously reported (Mortlock et al., 2003). Images were taken using an inverted microscope (1X71; Olympus) equipped with a digital camera (DP71; Olympus) and were imported into Photoshop (Adobe), where they were formatted without using any imaging enhancement. For cryosectioning, whole mount stained embryos were cryoembedded in optimal cutting temperature compound (Sakura). 50-μm sections were warm adhered on Superfrost-Plus slides (Fisher Scientific), washed thoroughly, and mounted using Aqua-Polymount (Polysciences). Section images were taken using the IX71 microscope with DP71 digital camera. Sections subjected to immunofluorescence were imaged using a microscope (Axiophot; Carl Zeiss MicroImaging, Inc.) with a camera (Micromax; Princeton Instruments), and images were imported into Photoshop for formatting.

Micromass cultures, in vitro conditional inactivation of TβRII, X-galactosidase histochemical staining, and affinity labeling with ^{125}I–TGF-β1

Limb bud mesenchymal cells from E11.5 embryos were isolated and micromass cultured as described previously (Cash et al., 1997). To conditionally inactivate TβRII, micromasses from *Tgfbr2*$^{flox/flox}$ or *Tgfbr2*$^{flox/flox}$*-R26R* embryos were infected either with HR-MMPCreGFP or MMP-GFP retroviral vectors as previously reported to generate Cre^{+}Tgfbr2^{KO} micromasses or MMP^{+}Tgfbr2$^{flox/flox}$ micromasses, respectively (Silver and Livingston, 2001; Longobardi et al., 2006). Infections were performed 1, 24, and 48 h after seeding. ^{125}I–TGF-β1–TβR affinity cross-linking was performed as previously reported (Longobardi et al., 2006).

WIB analysis and quantitative real-time PCR

Cell lysates and total RNA were obtained as previously reported from Cre^{+}Tgfbr2^{KO} micromasses or MMP^{+}Tgfbr2$^{flox/flox}$ micromasses cultured for 36 h and were treated with or without 20 ng/ml TGF-β (Longobardi et al., 2006). Treatment was repeated after 24 h, and cells were harvested 12 h later (total TGF-β treatment time was 36 h); WIB analysis was performed as previously reported (Longobardi et al., 2006). Noggin and phospho-Smad-1/-5/-8 polyclonal antibodies were obtained from Cell Signaling, and anti–β-actin antibody was purchased from Sigma-Aldrich. WIB images were semiautomatically analyzed using a custom-built densitometric image analysis code in MATLAB (Mathworks). Quantitative RT-PCR was performed as previously described (Longobardi et al., 2006). PCR primers for *Noggin* amplification were 5′-AAGGAGAAGGATCTGAACGAGACG-3′ and 5′-TCGGAGAACTCCAGCCCTTTGAT-3′.

Tgfbr2 deletion by genomic DNA analysis

LCM was performed as previously described (Bhowmick et al., 2004). In brief, E16.5 autopod paraffin sections (5 μm on uncharged slides) were immediately subjected to LCM on an LCM system (PixCell IIe; Arcturus). The captured cells were subsequently extracted for DNA amplification to determine the recombination of Tgfbr2 exon 2 by PRC as previously described (Bhowmick et al., 2004). Genomic DNA was also obtained from E17.5 Tgfbr2^{Prx1KO} and Tgfbr2$^{flox/flox}$ forelimb- and hindlimb-dissected digit bones and interphalangeal joints after removal of the skin and surrounding tissues and was subjected to quantitative real-time PCR using previously reported primers (Chytil et al., 2002; Baffi et al., 2004).

Statistical analysis

Data are presented as mean ± SD and are analyzed using an unpaired *t* test or one-way analysis of variance (Sigmastat Software; Sigma-Aldrich). Statistical significance was set at $P < 0.05$.

Online supplemental material

Fig. S1 shows recombination of the TβRII exon 2 in the joints by LCM followed by PCR. Fig. S2 shows the recombination of Tgfr2 in Cre^{+}Tgfbr2^{KO} and in Cre^{+}Tgfbr2^{KO}-R26R micromass cultures. Fig. S3 shows a schematic diagram of the *Tgfbr2-GFP-β−GEO-BAC* reporter construct. Online supplemental material is available at http://www.jcb.org/cgi/content/full/jcb.200611031/DC1.

We thank C.J. Tabin, P. Soriano, R.M. Harland, D.P. Silver, S.K. Dey, D.M. Kingsley, A. McMahon, and H. Kronenberg for providing animals or reagents. We acknowledge the support of the Vanderbilt Cell Imaging Shared Resource and the Vanderbilt Transgenic Core Facility.

This work was supported by an Arthritis Foundation Investigator Award and by National Institutes of Health grant 5R01DK070929-02 to A. Spagnoli.

Submitted: 8 November 2006
Accepted: 21 May 2007

References

Ando, K., S. Kanazawa, T. Tetsuka, S. Ohta, X. Jiang, T. Tada, M. Kobayashi, N. Matsui, and T. Okamoto. 2003. Induction of Notch signaling by tumor necrosis factor in rheumatoid synovial fibroblasts. *Oncogene*. 22:7796–7803.

Antonopoulou, I., L.A. Mavrogiannis, A.O. Wilkie, and G.M. Morriss-Kay. 2004. Alx4 and Msx2 play phenotypically similar and additive roles in skull vault differentiation. *J. Anat.* 204:487–499.

Archer, C.W., G.P. Dowthwaite, and P. Francis-West. 2003. Development of synovial joints. *Birth Defects Res. C. Embryo Today*. 69:144–155.

Baffi, M.O., E. Slattery, P. Sohn, H.L. Moses, A. Chytil, and R. Serra. 2004. Conditional deletion of the TGF-beta type II receptor in Col2a expressing cells results in defects in the axial skeleton without alterations in chondrocyte differentiation or embryonic development of long bones. *Dev. Biol.* 276:124–142.

Bhowmick, N.A., A. Chytil, D. Plieth, A.E. Gorska, N. Dumont, S. Shappell, M.K. Washington, E.G. Neilson, and H.L. Moses. 2004. TGF-beta signaling in fibroblasts modulates the oncogenic potential of adjacent epithelia. *Science*. 303:848–851.

Blokzijl, A., C. Dahlqvist, E. Reissmann, A. Falk, A. Moliner, U. Lendahl, and C.F. Ibanez. 2003. Cross-talk between the Notch and TGF-β signaling pathways mediated by interaction of the Notch intracellular domain with Smad3. *J. Cell Biol.* 163:723–728.

Brunet, L.J., J.A. McMahon, A.P. McMahon, and R.M. Harland. 1998. Noggin, cartilage morphogenesis, and joint formation in the mammalian skeleton. *Science*. 280:1455–1457.

Cash, D.E., C.B. Bock, K. Schughart, E. Linney, and T.M. Underhill. 1997. Retinoic acid receptor alpha function in vertebrate limb skeletogenesis: a modulator of chondrogenesis. *J. Cell Biol.* 136:445–457.

Chen, X., C.M. Macica, B.E. Dreyer, V.E. Hammond, J.R. Hens, W.M. Philbrick, and A.E. Broadus. 2006. Initial characterization of PTH-related protein gene-driven lacZ expression in the mouse. *J. Bone Miner. Res.* 21:113–123.

Chytil, A., M.A. Magnuson, C.V. Wright, and H.L. Moses. 2002. Conditional inactivation of the TGF-beta type II receptor using Cre:Lox. *Genesis*. 32:73–75.

Das, S.K., H. Lim, J. Wang, B.C. Paria, M. BazDresch, and S.K. Dey. 1997. Inappropriate expression of human transforming growth factor (TGF)-alpha in the uterus of transgenic mouse causes downregulation of TGF-beta receptors and delays the blastocyst-attachment reaction. *J. Mol. Endocrinol*. 18:243–257.

Deal, K.K., V.A. Cantrell, R.L. Chandler, T.L. Saunders, D.P. Mortlock, and E.M. Southard-Smith. 2006. Distant regulatory elements in a Sox10-betaGEO BAC transgene are required for expression of Sox10 in the enteric nervous system and other neural crest-derived tissues. *Dev. Dyn.* 235:1413–1432.

DiLeone, R.J., G.A. Marcus, M.D. Johnson, and D.M. Kingsley. 2000. Efficient studies of long-distance Bmp5 gene regulation using bacterial artificial chromosomes. *Proc. Natl. Acad. Sci. USA*. 97:1612–1617.

Dowthwaite, G.P., J.C. Bishop, S.N. Redman, I.M. Khan, P. Rooney, D.J. Evans, L. Haughton, Z. Bayram, S. Boyer, B. Thomson, et al. 2004. The surface of articular cartilage contains a progenitor cell population. *J. Cell Sci.* 117:889–897.

Dunker, N., and K. Krieglstein. 2000. Targeted mutations of transforming growth factor-beta genes reveal important roles in mouse development and adult homeostasis. *Eur. J. Biochem.* 267:6982–6988.

Ganan, Y., D. Macias, M. Duterque-Coquillaud, M.A. Ros, and J.M. Hurle. 1996. Role of TGF betas and BMPs as signals controlling the position of the digits and the areas of interdigital cell death in the developing chick limb autopod. *Development*. 122:2349–2357.

Gazzerro, E., V. Gangji, and E. Canalis. 1998. Bone morphogenetic proteins induce the expression of noggin, which limits their activity in cultured rat osteoblasts. *J. Clin. Invest.* 102:2106–2114.

Gong, Y., D. Krakow, J. Marcelino, D. Wilkin, D. Chitayat, R. Babul-Hirji, L. Hudgins, C.W. Cremers, F.P. Cremers, H.G. Brunner, et al. 1999. Heterozygous mutations in the gene encoding noggin affect human joint morphogenesis. *Nat. Genet.* 21:302–304.

Hartmann, C., and C.J. Tabin. 2001. Wnt-14 plays a pivotal role in inducing synovial joint formation in the developing appendicular skeleton. *Cell*. 104:341–351.

Hayes, A.J., G.P. Dowthwaite, S.V. Webster, and C.W. Archer. 2003. The distribution of Notch receptors and their ligands during articular cartilage development. *J. Anat.* 202:495–502.

Ishii, M., A.E. Merrill, Y.S. Chan, I. Gitelman, D.P. Rice, H.M. Sucov, and R.E. Maxson Jr. 2003. Msx2 and Twist cooperatively control the development of the neural crest-derived skeletogenic mesenchyme of the murine skull vault. *Development*. 130:6131–6142.

Ito, Y., J.Y. Yeo, A. Chytil, J. Han, P. Bringas Jr., A. Nakajima, C.F. Shuler, H.L. Moses, and Y. Chai. 2003. Conditional inactivation of Tgfbr2 in cranial neural crest causes cleft palate and calvaria defects. *Development*. 130:5269–5280.

Kaartinen, V., J.W. Voncken, C. Shuler, D. Warburton, D. Bu, N. Heisterkamp, and J. Groffen. 1995. Abnormal lung development and cleft palate in mice lacking TGF-beta 3 indicates defects of epithelial-mesenchymal interaction. *Nat. Genet.* 11:415–421.

Lawler, S., A.F. Candia, R. Ebner, L. Shum, A.R. Lopez, H.L. Moses, C.V. Wright, and R. Derynck. 1994. The murine type II TGF-beta receptor has a coincident embryonic expression and binding preference for TGF-beta 1. *Development*. 120:165–175.

Lee, E.C., D. Yu, J. Martinez de Velasco, L. Tessarollo, D.A. Swing, D.L. Court, N.A. Jenkins, and N.G. Copeland. 2001. A highly efficient *Escherichia coli*-based chromosome engineering system adapted for recombinogenic targeting and subcloning of BAC DNA. *Genomics*. 73:56–65.

Logan, M., J.F. Martin, A. Nagy, C. Lobe, E.N. Olson, and C.J. Tabin. 2002. Expression of Cre Recombinase in the developing mouse limb bud driven by a Prxl enhancer. *Genesis*. 33:77–80.

Longobardi, L., L. O'Rear, S. Aakula, B. Johnstone, K. Shimer, A. Chytil, W.A. Horton, H.L. Moses, and A. Spagnoli. 2006. Effect of IGF-I in the chondrogenesis of bone marrow mesenchymal stem cells in the presence or absence of TGF-beta signaling. *J. Bone Miner. Res.* 21:626–636.

Mak, K.K., M.H. Chen, T.F. Day, P.T. Chuang, and Y. Yang. 2006. Wnt/beta-catenin signaling interacts differentially with Ihh signaling in controlling endochondral bone and synovial joint formation. *Development*. 133:3695–3707.

Metsaranta, M., D. Toman, B. De Crombrugghe, and E. Vuorio. 1991. Specific hybridization probes for mouse type I, II, III and IX collagen mRNAs. *Biochim. Biophys. Acta*. 1089:241–243.

Millan, F.A., F. Denhez, P. Kondaiah, and R.J. Akhurst. 1991. Embryonic gene expression patterns of TGF beta 1, beta 2 and beta 3 suggest different developmental functions in vivo. *Development*. 111:131–143.

Mortlock, D.P., L.C. Post, and J.W. Innis. 1996. The molecular basis of hypodactyly (Hd): a deletion in Hoxa 13 leads to arrest of digital arch formation. *Nat. Genet.* 13:284–289.

Mortlock, D.P., C. Guenther, and D.M. Kingsley. 2003. A general approach for identifying distant regulatory elements applied to the Gdf6 gene. *Genome Res.* 13:2069–2081.

Mountford, P., B. Zevnik, A. Duwel, J. Nichols, M. Li, C. Dani, M. Robertson, I. Chambers, and A. Smith. 1994. Dicistronic targeting constructs: reporters and modifiers of mammalian gene expression. *Proc. Natl. Acad. Sci. USA*. 91:4303–4307.

Oshima, M., H. Oshima, and M.M. Taketo. 1996. TGF-beta receptor type II deficiency results in defects of yolk sac hematopoiesis and vasculogenesis. *Dev. Biol.* 179:297–302.

Pacifici, M., E. Koyama, Y. Shibukawa, C. Wu, Y. Tamamura, M. Enomoto-Iwamoto, and M. Iwamoto. 2006. Cellular and molecular mechanisms of synovial joint and articular cartilage formation. *Ann. NY Acad. Sci.* 1068:74–86.

Pelton, R.W., M.D. Johnson, E.A. Perkett, L.I. Gold, and H.L. Moses. 1991a. Expression of transforming growth factor-beta 1, -beta 2, and -beta 3 mRNA and protein in the murine lung. *Am. J. Respir. Cell Mol. Biol.* 5:522–530.

Pelton, R.W., B. Saxena, M. Jones, H.L. Moses, and L.I. Gold. 1991b. Immunohistochemical localization of TGFβ1, TGFβ2, and TGFβ3 in the mouse embryo: expression patterns suggest multiple roles during embryonic development. *J. Cell Biol.* 115:1091–1105.

Rohrer, F. 1921. Der Index der korperpirlle als Mass des Ernahrungszustandes [Index of state of nutrition]. *Munch. Med. Wochenschr.* 68:580–582.

Sanford, L.P., I. Ormsby, A.C. Gittenberger-de Groot, H. Sariola, R. Friedman, G.P. Boivin, E.L. Cardell, and T. Doetschman. 1997. TGFbeta2 knockout mice have multiple developmental defects that are non-overlapping with other TGFbeta knockout phenotypes. *Development*. 124:2659–2670.

Seemann, P., R. Schwappacher, K.W. Kjaer, D. Krakow, K. Lehmann, K. Dawson, S. Stricker, J. Pohl, F. Ploger, E. Staub, et al. 2005. Activating and deactivating mutations in the receptor interaction site of GDF5 cause symphalangism or brachydactyly type A2. *J. Clin. Invest.* 115:2373–2381.

Serra, R., and C. Chang. 2003. TGF-beta signaling in human skeletal and patterning disorders. *Birth Defects Res. C. Embryo Today*. 69:333–351.

Serra, R., M. Johnson, E.H. Filvaroff, J. LaBorde, D.M. Sheehan, R. Derynck, and H.L. Moses. 1997. Expression of a truncated, kinase-defective TGF-β type II receptor in mouse skeletal tissue promotes terminal chondrocyte differentiation and osteoarthritis. *J. Cell Biol.* 139:541–552.

Shull, M.M., I. Ormsby, A.B. Kier, S. Pawlowski, R.J. Diebold, M. Yin, R. Allen, C. Sidman, G. Proetzel, D. Calvin, et al. 1992. Targeted disruption of the mouse transforming growth factor-beta 1 gene results in multifocal inflammatory disease. *Nature*. 359:693–699.

Silver, D.P., and D.M. Livingston. 2001. Self-excising retroviral vectors encoding the Cre recombinase overcome Cre-mediated cellular toxicity. *Mol. Cell*. 8:233–243.

Sirard, C., J.L. de la Pompa, A. Elia, A. Itie, C. Mirtsos, A. Cheung, S. Hahn, A. Wakeham, L. Schwartz, S.E. Kern, et al. 1998. The tumor suppressor gene Smad4/Dpc4 is required for gastrulation and later for anterior development of the mouse embryo. *Genes Dev.* 12:107–119.

Soriano, P. 1999. Generalized lacZ expression with the ROSA26 Cre reporter strain. *Nat. Genet.* 21:70–71.

Spater, D., T.P. Hill, R.J. Sullivan, M. Gruber, D.A. Conner, and C. Hartmann. 2006. Wnt9a signaling is required for joint integrity and regulation of Ihh during chondrogenesis. *Development*. 133:3039–3049.

Storm, E.E., and D.M. Kingsley. 1996. Joint patterning defects caused by single and double mutations in members of the bone morphogenetic protein (BMP) family. *Development*. 122:3969–3979.

Storm, E.E., and D.M. Kingsley. 1999. GDF5 coordinates bone and joint formation during digit development. *Dev. Biol.* 209:11–27.

Storm, E.E., T.V. Huynh, N.G. Copeland, N.A. Jenkins, D.M. Kingsley, and S.J. Lee. 1994. Limb alterations in brachypodism mice due to mutations in a new member of the TGF beta-superfamily. *Nature*. 368:639–643.

Takahashi, T., I. Takahashi, M. Komatsu, Y. Sawaishi, K. Higashi, G. Nishimura, H. Saito, and G. Takada. 2001. Mutations of the NOG gene in individuals with proximal symphalangism and multiple synostosis syndrome. *Clin. Genet.* 60:447–451.

Warming, S., N. Costantino, D.L. Court, N.A. Jenkins, and N.G. Copeland. 2005. Simple and highly efficient BAC recombineering using galK selection. *Nucleic Acids Res.* 33:e36.

Weinstein, M., X. Yang, C. Li, X. Xu, J. Gotay, and C.X. Deng. 1998. Failure of egg cylinder elongation and mesoderm induction in mouse embryos lacking the tumor suppressor smad2. *Proc. Natl. Acad. Sci. USA*. 95:9378–9383.

Wuyts, W., E. Cleiren, T. Homfray, A. Rasore-Quartino, F. Vanhoenacker, and W. Van Hul. 2000a. The ALX4 homeobox gene is mutated in patients with ossification defects of the skull (foramina parietalia permagna, OMIM 168500). *J. Med. Genet.* 37:916–920.

Wuyts, W., W. Reardon, S. Preis, T. Homfray, A. Rasore-Quartino, H. Christians, P.J. Willems, and W. Van Hul. 2000b. Identification of mutations in the MSX2 homeobox gene in families affected with foramina parietalia permagna. *Hum. Mol. Genet.* 9:1251–1255.

Yang, X., L. Chen, X. Xu, C. Li, C. Huang, and C.X. Deng. 2001. TGF-beta/Smad3 signals repress chondrocyte hypertrophic differentiation and are required for maintaining articular cartilage. *J. Cell Biol.* 153:35–46.

Zhu, Y., J.A. Richardson, L.F. Parada, and J.M. Graff. 1998. Smad3 mutant mice develop metastatic colorectal cancer. *Cell*. 94:703–714.